

Electronic Supplementary Information

Study of DNA/BSA interaction and catalytic potential of oxidovanadium(V) complexes with ONO donor ligands

Subhashree P. Dash,^{a,b1} Alok K. Panda,^{c1} Sarita Dhaka,^{d1} Sagarika Pasayat,^a Ashis Biswas,^c Mannar R. Maurya,^d Paresh Kumar Majhi,^{a,e} Aurélien Crochet^f and Rupam Dinda^{*a}

^aDepartment of Chemistry, National Institute of Technology, Rourkela 769008, Odisha, India

^bDepartment of Chemistry, Indira Gandhi Institute of Technology, Sarang, Parjang, Dhenkanal 759146, India

^cSchool of Basic Science, Indian Institute of Technology Bhubaneswar, Bhubaneswar 751 013, Odisha, India.

^dDepartment of Chemistry, Indian Institute of Technology Roorkee, Roorkee 247667, India

^eInstitute for Chemical Research, Kyoto University, Gokasho Uji, Kyoto 611-0011, Japan

^fFribourg Center for Nanomaterials, Department of Chemistry, University of Fribourg, CH-1700 Fribourg, Switzerland

¹The authors contribute equally to this work

Experimental Section

(a) X-ray Crystallography

Single crystals of compounds, were mounted on Bruker Smart Apex CCD diffractometer (**2**) equipped with a graphite monochromator and Stoe IPDS 2 diffractometer (**5**) equipped with an Oxford Cryosystem open flow cryostat and a Mo K α radiator (λ) 0.71073 Å. Crystallographic data and details of refinement are given in Table S1. The unit cell dimensions and intensity data were measured at 293(2) K. Absorption correction was partially integrated in the data reduction procedure for crystals of **5**.³⁶ The intensity data were corrected for Lorentz, polarization and absorption effects. Absorption corrections were applied using SADABS and the structures were solved by direct methods using the program SHELXS-97³⁷ and refined using least squares with the SHELXL-97³⁷ software program. Hydrogens were either found or placed in calculated positions and isotropically refined using a riding model. The non-hydrogen atoms were refined anisotropically.

(b) Absorption spectral studies

The UV-vis absorption titration experiments were performed against a fixed concentration of metal complex (25 μ M) and varying the CT-DNA concentration from 0 to 65 μ M. After each addition of CT-DNA (5 μ M) to the metal complex, the spectra were recorded using Perkin Elmer Lambda35 spectrophotometer. The data were then fit to the following equation to obtain binding constant K_b .^{32e}

$$\frac{[DNA]}{\epsilon_a - \epsilon_f} = \frac{[DNA]}{\epsilon_b - \epsilon_f} + \frac{1}{K_b(\epsilon_b - \epsilon_f)}; \quad \text{Eq. 1}$$

where [DNA] is the concentration of DNA base pairs, ϵ_a , ϵ_f and ϵ_b correspond to apparent extinction co-efficient for the complex *i.e.* Abs/[complex] in presence of DNA, in absence of DNA and to fully bound DNA respectively. A plot of [DNA]/($\epsilon_a - \epsilon_f$) vs [DNA] gave a slope and the intercept equal to $1/(\epsilon_b - \epsilon_f)$ and $1/K_b(\epsilon_b - \epsilon_f)$, respectively. The binding constant K_b was calculated from the ratio of the slope to the intercept. Binding of ligands to CT-DNA was also studied. For this, a fixed concentration of ligand [25 μ M in 10 mM Tris-HCl buffer (pH 8.0) containing 1% DMF] was titrated with variable DNA concentration ranging from 0 to 250 μ M.

(c) Competitive DNA binding fluorescence measurements

The DNA binding probes, 4',6-diamidino-2-phenylindole (DAPI) and methyl green (MG), binds to the minor and major groove of the DNA respectively,³⁹ while ethidium bromide (EB), binds to DNA by intercalation.³⁹ Briefly, each of the DNA binding probe *i.e.* DAPI, MG and EB, 2 μ M each were incubated with 50 μ M of CT-DNA for 1 h at 25 °C. Thereafter, the competitive binding of the complexes **1–5** with DAPI, MG and EB bound CT-DNA was studied by measuring the fluorescence intensities of the DAPI, MG and EB bound CT-DNA with increasing concentration of the complexes. The fluorescence emission intensities of DAPI, MG and EB at 455 nm (excitation 358 nm), 672 nm (excitation 633 nm) and 597

nm (excitation 510 nm) respectively, was monitored with an increasing amount of the complex concentration (0–90 μ M) with the aid of Fluoromax 4P spectrofluorimeter (Horiba Jobin Mayer, USA).

(d) Photo-induced DNA cleavage

The photo cleavage reactions were carried out under illuminated conditions using UVA source at 350 nm (Luzchem Photoreactor Model LZC-1, Ontario, Canada) fitted with 14 UVA tubes for 3 h at room temperature. After photo irradiation, each sample was further incubated for 1.0 h at 37 °C and analyzed for the photo cleaved products using gel electrophoresis. DNA cleavage was indicated by the decrease in the supercoiled pUC19 DNA (Form I) and subsequent formation of nicked circular DNA (Form II) and linearized DNA (Form III). Bands were visualized by UV light (302nm) and photographed. The extent of SC DNA cleavage was measured from the intensities of the bands using UVP (Gel Doc It²) Gel Documentation System. The corrections were made for the low level of nicked circular (NC) form of DNA present in the original SC DNA sample and for the low affinity of EB binding to SC compared to NC and linear forms of DNA.⁴¹ The percentage of net DNA cleavage was calculated by the following equation:

$$\text{Net DNA cleavage \%} = \frac{\text{Form II}_s + 2 \times \text{Form III}_s}{\text{Form I}_s + \text{Form II}_s + 2 \times \text{Form III}_s} - \frac{\text{Form II}_c + 2 \times \text{Form III}_c}{\text{Form I}_c + \text{Form II}_c + 2 \times \text{Form III}_c} \quad \text{Eq.2}$$

The subscripts “s” and “c” refers to the sample and control respectively.^{32e} Appropriate DNA controls were taken to calculate the net DNA cleavage percent. The observed error in measuring the band intensities ranged between 3% – 6%. The mechanistic studies were performed using two singlet oxygen quenchers (sodium azide and L-histidine) and two hydroxyl radical quenchers (KI and D-mannitol). The quenchers were added to the DNA solution prior to the addition of the complexes. The concentration of each quencher was 0.5 mM.

(e) Bovine serum albumin (BSA) interaction studies

Stern-Volmer plots and Scatchard analysis were done using corrected fluorescence data taking into account the effect of dilution. Linear fit of the data using the Stern-Volmer equation (Eq.3),

$$\frac{F_0}{F} = 1 + K_{SV}[Q] \quad \text{Eq.3}$$

and the Scatchard equation (Eq.4),

$$\log \left[\frac{F_0 - F}{F} \right] = \log K_{BSA} + n \log [Q] \quad \text{Eq.4}$$

where F_0 and F are the emission intensity of BSA in absence and in presence of the quencher (complexes) concentration $[Q]$ respectively, gave the Stern-Volmer quenching constant (K_{SV}), the binding constant (K_{BSA}) and the number of binding sites (n).⁴⁰

Table of Contents

Table S1 Crystal data and refinement details for **2** and **5**

Table S2 Selected bond distances (Å) and angles (°) for **2** and **5**

Table S3 Binding constant (K_b) values for the "CT-DNA-ligand" interactions^a

Table S4 Results of oxidative bromination of salicylaldehyde catalyzed by **3** after 3 h of contact time

Table S5 Conversion of methyl phenyl sulfide (0.620 g, 5 mmol) using **3** as catalyst in 2.5 h of reaction time under different reaction conditions

Fig. S1 Absorption spectral traces of the complexes **1** (a), **2** (b), **3** (c), **4** (d) and **5** (e) (25 μ M each) in 10 mM Tris-HCl buffer (pH 8.0) containing 1% DMF after 0, 12, 24 and 72 h.

Fig. S2 Electronic absorption spectra for H_2L^1 (a), H_2L^2 (b), H_2L^3 (c) and H_2L^4 (d) (25 μ M each) upon the titration of CT-DNA (0 – 250 μ M) in 10 mM Tris-HCl buffer (pH 8.0) containing 1% DMF. The inset shows the linear fit of $[DNA]/(\epsilon_a - \epsilon_f)$ vs $[DNA]$ from which the binding constant (K_b) was calculated using Eq. 1 (see main text).

Fig. S3 Circular dichroism spectra of CT-DNA (150 μ M) in the presence and absence complexes **1–5** (25 μ M) in 10 mM Tris-HCl buffer (pH 8.0) containing 1% DMF. The path length of the cuvette was 10 mm.

Fig. S4 Fluorescence emission spectra of DAPI (2 μ M) bound to CT-DNA (50 μ M) in the presence of complexes **1** (a), **2** (b), **3** (c), **4** (d) and **5** (e) (0–90 μ M) in 10 mM Tris-HCl buffer (pH 8.0) containing 1% DMF. The arrow indicates the effect of increasing the concentration of the complex on the fluorescence emission of DAPI bound CT-DNA. The excitation and emission band width were 2.5 and 5.0 nm respectively.

Fig. S5 Fluorescence emission spectra of MG (2 μ M) bound to CT-DNA (50 μ M) in the presence of complexes **1** (a), **2** (b), **3** (c), **4** (d) and **5** (e) (0–90 μ M) in 10 mM Tris-HCl buffer (pH 8.0) containing 1% DMF. The arrow indicates the effect of increasing the concentration of the complex on the fluorescence emission of MG bound CT-DNA. The excitation and emission band width were 5 and 10.0 nm respectively.

Fig. S6 Fluorescence emission spectra of ethidium bromide (EB) (2 μ M) bound to CT-DNA (50 μ M) in the presence of complex **1** (a), **2** (b), **3** (c), **4** (d) and **5** (e) (0 – 90 μ M) in 10 mM Tris-HCl buffer (pH 8.0) containing 1% DMF. The arrow indicates the effect of increasing the concentration of the complex on the fluorescence emission of EB bound CT-DNA. The excitation and emission band width were 2.5 and 5.0 nm respectively.

Fig. S7 Gel diagram showing concentration dependent DNA cleavage by **1–5**; 300 ng of SC pUC19 DNA at different concentrations of the complexes [1–500 μ M in 50 mM Tris-HCl buffer (pH 8.0) containing 1% DMF] was photo-irradiated with UVA at 350 nm for 3 h. Lanes **1–9**: 1, 2.5, 5.0, 7.5, 10, 50, 75, 100 and 500 μ M of **1–5**.

Fig. S8 Effect of DMF (1%) and ligands on the photo-induced cleavage of SC pUC19 DNA. 300 ng SC pUC19 DNA was photo-irradiated in absence and presence of 1% DMF and various ligands (100 μ M) with UVA at 350 nm for 3 h. Lane 1, DNA only; Lane 2, DNA in presence of 1% DMF; Lane 3, DNA + $\mathbf{H}_2\mathbf{L}^1$; Lane 4, DNA + $\mathbf{H}_2\mathbf{L}^2$; Lane 5, DNA + $\mathbf{H}_2\mathbf{L}^3$; Lane 6, DNA + $\mathbf{H}_2\mathbf{L}^4$.

Fig. S9 Gel diagram depicting cleavage of SC pUC19 DNA by **1–5** in presence of various additives in 50 mM Tris-HCl buffer (pH 8.0) containing 1% DMF. SC pUC19 DNA (300 ng) in the presence of various additives was photo-irradiated at 350 nm for 3 h with **1–5** (100 μ M). The additive concentrations were: sodium azide (0.5 mM), L-histidine (0.5 mM), KI (0.5 mM) and D-mannitol (0.5 mM). Lane 1, DNA + complex; Lane 2, DNA + complex + sodium azide; Lane 3, DNA + complex + L-histidine; Lane 4, DNA + complex + KI; Lane 5, DNA + complex + D-mannitol.

Fig. S10 DNA cleavage of SC pUC19 DNA by **1–5** in presence of various additives in 50 mM Tris-HCl buffer (pH 8.0) containing 1% DMF. SC pUC19 DNA (300 ng) in the presence of various additives was photo-irradiated at 350 nm for 3 h with **1–5** (100 μ M). The additive concentrations were: sodium azide (0.5 mM), L-histidine (0.5 mM), KI (0.5 mM) and D-mannitol (0.5 mM).

Fig. S11 The plot represents the linear fit of $\log [(F_0-F)/F]$ vs $\log [Q]$ for **1** (a), **2** (b), **3** (c), **4** (d) and **5** (e) and the binding constant (K_{BSA}) was estimated using Eq.4. Here, [Q] stands for [quencher (complexes)].

Fig. S12 SDS-PAGE profile of concentration dependent photo-induced cleavage of BSA (5 μ M) in UVA light of 350 nm (84 W) for 90 min by **1** (a), **2** (b), **3** (c), **4** (d) and **5** (e). Lane 1, Molecular marker; Lane 2, BSA only; Lane 3, BSA + complex (1 μ M); Lane 4, BSA + complex (2.5 μ M); Lane 5, BSA + complex (5 μ M); Lane 6, BSA + complex (10 μ M); Lane 7, BSA + complex (50 μ M); Lane 8, BSA + complex (100 μ M); Lane 9, BSA + complex (300 μ M).

Fig. S13 Comparison of catalytic efficiency of different catalysts on the oxidative bromination of styrene. Reaction condition: styrene (1.04 g, 10 mmol), catalyst (0.0005g), 30 % aqueous H_2O_2 (3.39, 30 mmol), KBr (3.57 g, 30 mmol) and 70 % aqueous HClO_4 (2.86 g, 20 mmol).

Fig. S14 (a) Effect of catalyst amount on the oxidation of methyl phenyl sulfide. Reaction conditions: methyl phenyl sulfide (0.620 g, 5 mmol), 30 % H_2O_2 (1.14 g, 10 mmol) and acetonitrile (5 mL). (b) Effect of oxidant amount on the oxidation of methyl phenyl sulfide. Reaction conditions: methyl phenyl sulfide (0.620 g, 5 mmol), catalyst (0.001 g) and acetonitrile (5 mL). (c) Effect of solvent amount on the oxidation of methyl phenyl sulfide. Reaction conditions: methyl phenyl sulfide (0.620 g, 5 mmol), catalyst (0.001 g) and 30 % H_2O_2 (1.14 g, 10 mmol). (d) Effect of different catalyst (**1–5**) on oxidation of methyl phenyl sulfide.

Table S1 Crystal data and refinement details for **2** and **5**

Complex	2	5
Empirical formula	C ₂₀ H ₁₇ N ₂ O ₅ V	C ₅₀ H ₄₂ N ₆ O ₁₀ V ₂
Formula weight	416.30	988.77
Temperature	293(2) K	293(2) K
Wavelength	0.71073 Å	1.54184 Å
Crystal system	Monoclinic	Tetragonal
Space group	P 21/c	P 4/n
Unit cell dimensions	a = 18.249(3) Å b = 5.9376(11) Å c = 18.227(3) Å α = 90° β = 110.346(9)° γ = 90°	a = 21.5608(3) Å b = 21.5608(3) Å c = 10.1344(3) Å α = 90° β = 90° γ = 90°
Volume	1851.8(6) Å ³	4711.16(19) Å ³
Z	4	4
Density (calculated)	1.493 Mg/m ³	1.394 Mg/m ³
Absorption coefficient	0.571 mm ⁻¹	3.872 mm ⁻¹
F(000)	856	2040
Theta range for data collection	2.26 to 26.00°.	11.203 to 66.586°.
Reflections collected	26070	12627
Independent reflections	3645 [R(int) = 0.0979]	4129 [R(int) = 0.0317]
Completeness to theta = 25.00°	99.9 %	96.6 %
Refinement method	Full-matrix least-squares on F ²	Full-matrix least-squares on F ²
Data / restraints / parameters	3645 / 13 / 246	4129 / 0 / 310
Goodness-of-fit on F ²	1.056	1.011
Final R indices [I > 2σ(I)]	R1 = 0.0831, wR2 = 0.2028	R1 = 0.0457, wR2 = 0.1263
R indices (all data)	R1 = 0.1296, wR2 = 0.2560	R1 = 0.0532, wR2 = 0.1317

Table S2 Selected bond distances (Å) and angles (°) for **2** and **5**

Parameters	2	5
V(1)-O(1)	1.840(4)	1.853(1)
V(1)-O(2)	1.936(4)	1.966(1)
V(1)-O(3)	1.581(6)	1.601(2)
V(1)-O(4)	1.730(5)	1.779(2)
V(1)-N(1)	2.095(5)	2.110(2)
N(1)-N(2)	1.387(7)	1.393(2)
V(1)-N(3)		2.377(2)
O(1)-V(1)-O(3)	105.3(2)	100.89(7)
O(1)-V(1)-O(4)	98.6(2)	105.17(6)
O(1)-V(1)-N(1)	81.6(2)	82.09(6)
O(2)-V(1)-O(3)	104.4(2)	97.61(7)
O(2)-V(1)-O(4)	90.5(2)	91.29(6)
O(2)-V(1)-N(1)	74.7(2)	74.87(6)
O(3)-V(1)-O(4)	108.5(3)	102.04(7)
O(3)-V(1)-N(1)	98.4(2)	96.81(7)
O(3)-V(1)-N(3)		175.58(7)
O(1)-V(1)-N(3)		82.12(6)
O(4)-V(1)-N(3)		80.14(6)
O(2)-V(1)-N(3)		78.44(6)

Ligand	Binding constant (K_b) (M^{-1})
H₂L¹	2.53×10^3
H₂L²	1.21×10^4
H₂L³	9.11×10^3
H₂L⁴	3.96×10^4

Table S3 Binding constant (K_b) values for the "CT-DNA-ligand" interactions^a

^a The DNA binding constant was determined by the UV-vis spectral method.

Table S4 Results of oxidative bromination of salicylaldehyde catalyzed by **3** after 3 h of contact time

Entry no.	Catalyst (g)	H ₂ O ₂ (g, mmol)	KBr (g, mmol)	HClO ₄ (g, mmol)	% Conversion
1	0.0005	1.14, 10	1.19, 10	1.43,10	63
2	0.0005	1.14, 10	1.19, 10	2.14, 15	88
3	0.0005	1.14, 10	1.19, 10	2.86, 20	98
4	0.0005	0.57, 05	1.19, 10	2.14, 15	65
5	0.0005	1.71, 15	1.19, 10	2.14, 15	99
6	0.0005	1.14, 10	0.59, 05	2.14, 15	48
7	0.0005	1.14, 10	1.78, 15	2.14, 15	99
8	0.0010	1.14, 10	1.19, 10	1.43,10	68
9	0.0015	1.14, 10	1.19, 10	1.43,10	73

Table S5 Conversion of methyl phenyl sulfide (0.620 g, 5 mmol) using **3** as catalyst in 2.5 h of reaction time under different reaction conditions

Entry No.	Catalyst [g]	H ₂ O ₂ [g, mmol]	CH ₃ CN [mL]	Conv. [%]
1	0.0005	1.14, 10	5	66
2	0.0010	1.14, 10	5	94
3	0.0015	1.14, 10	5	98
4	0.0010	0.57, 05	5	67
5	0.0010	1.71, 15	5	99
6	0.0010	1.14, 10	10	34
7	0.0010	1.14, 10	15	17

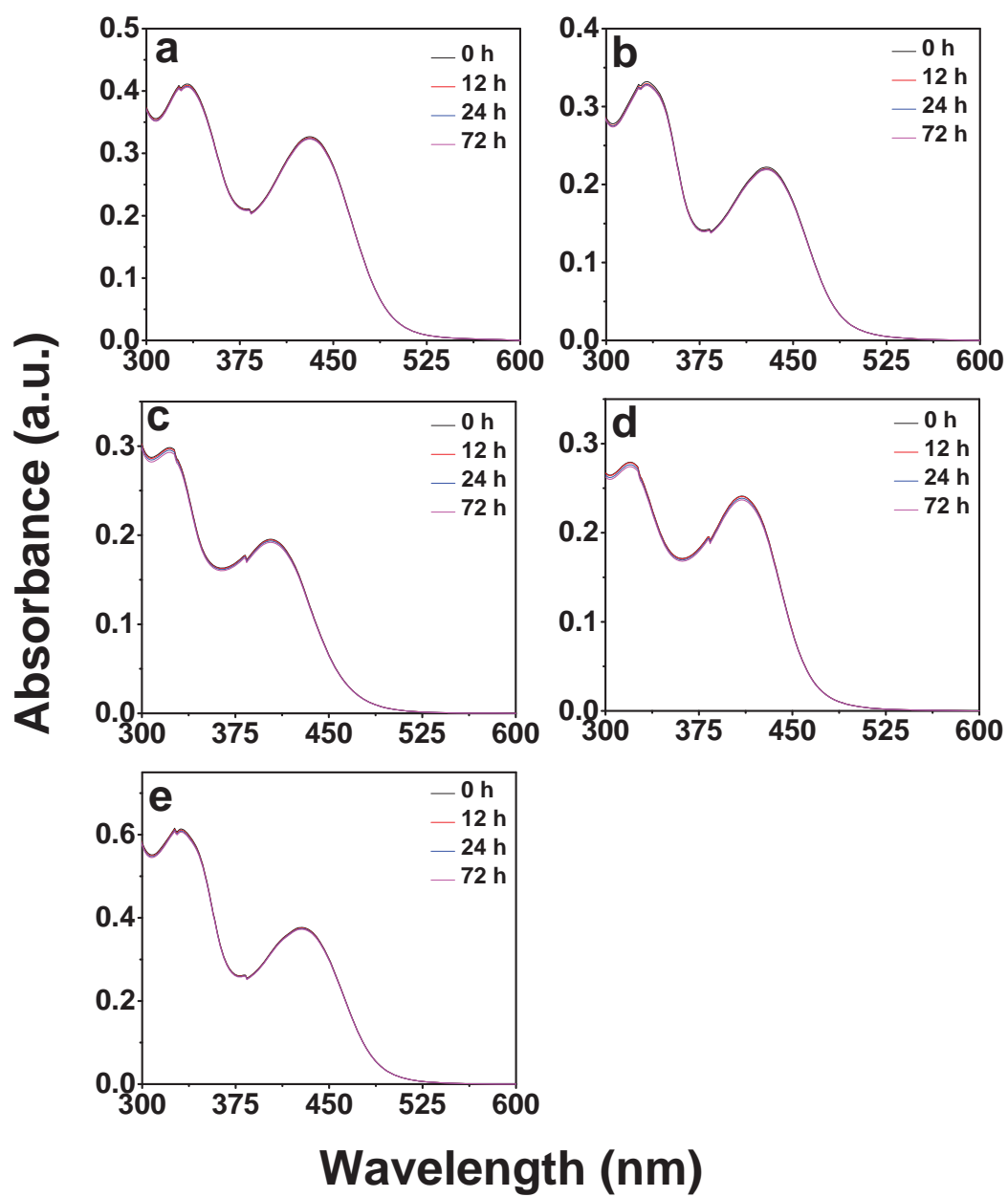


Fig. S1

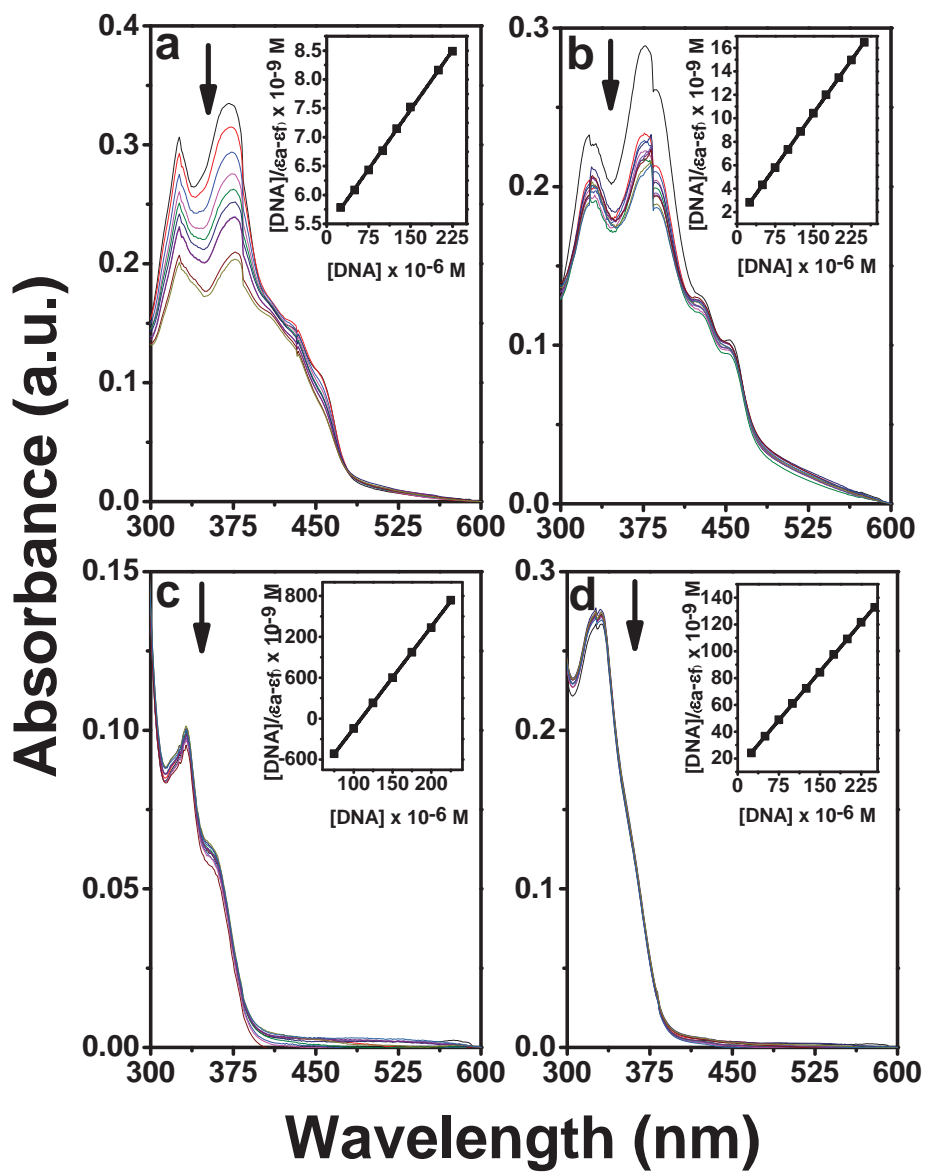


Fig. S2

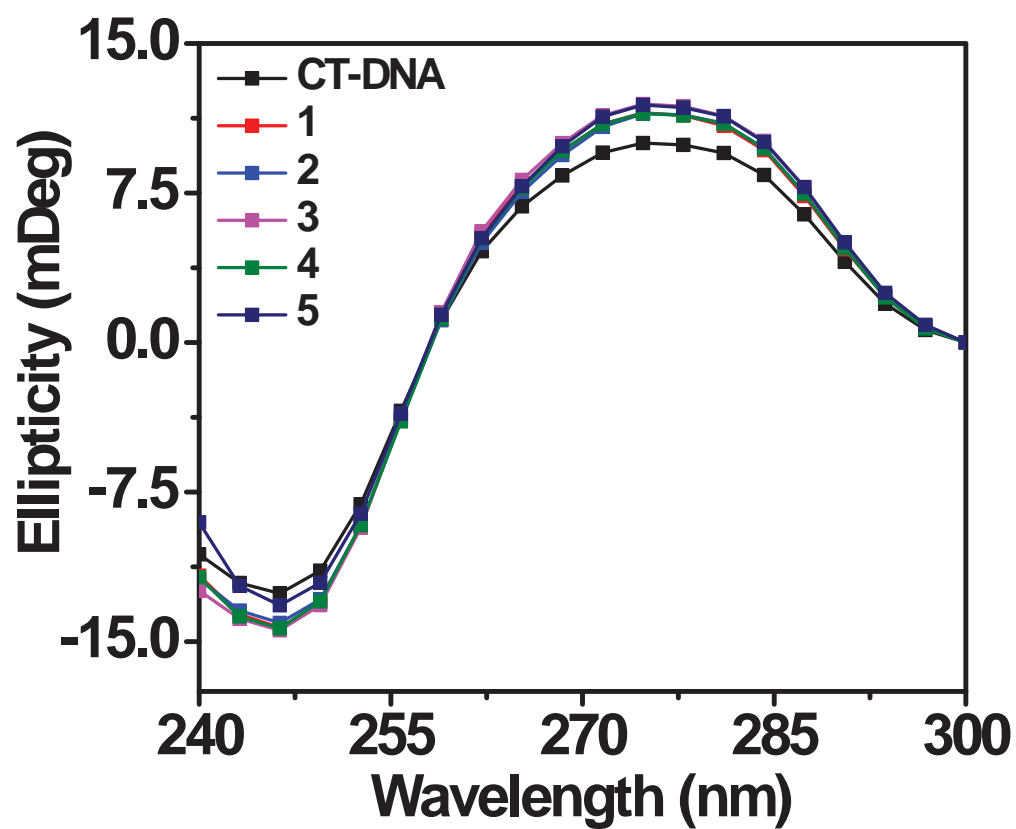


Fig. S3

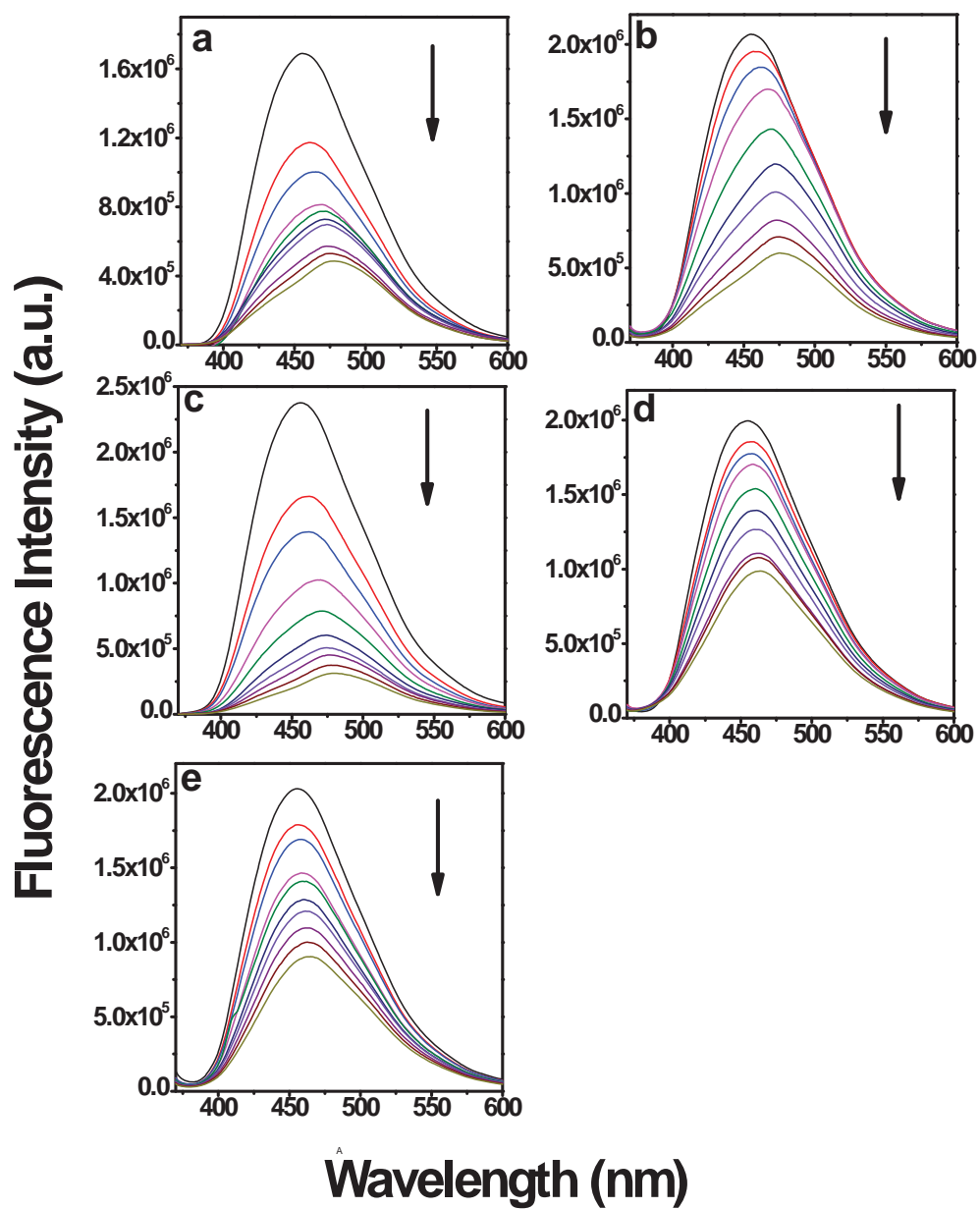


Fig. S4

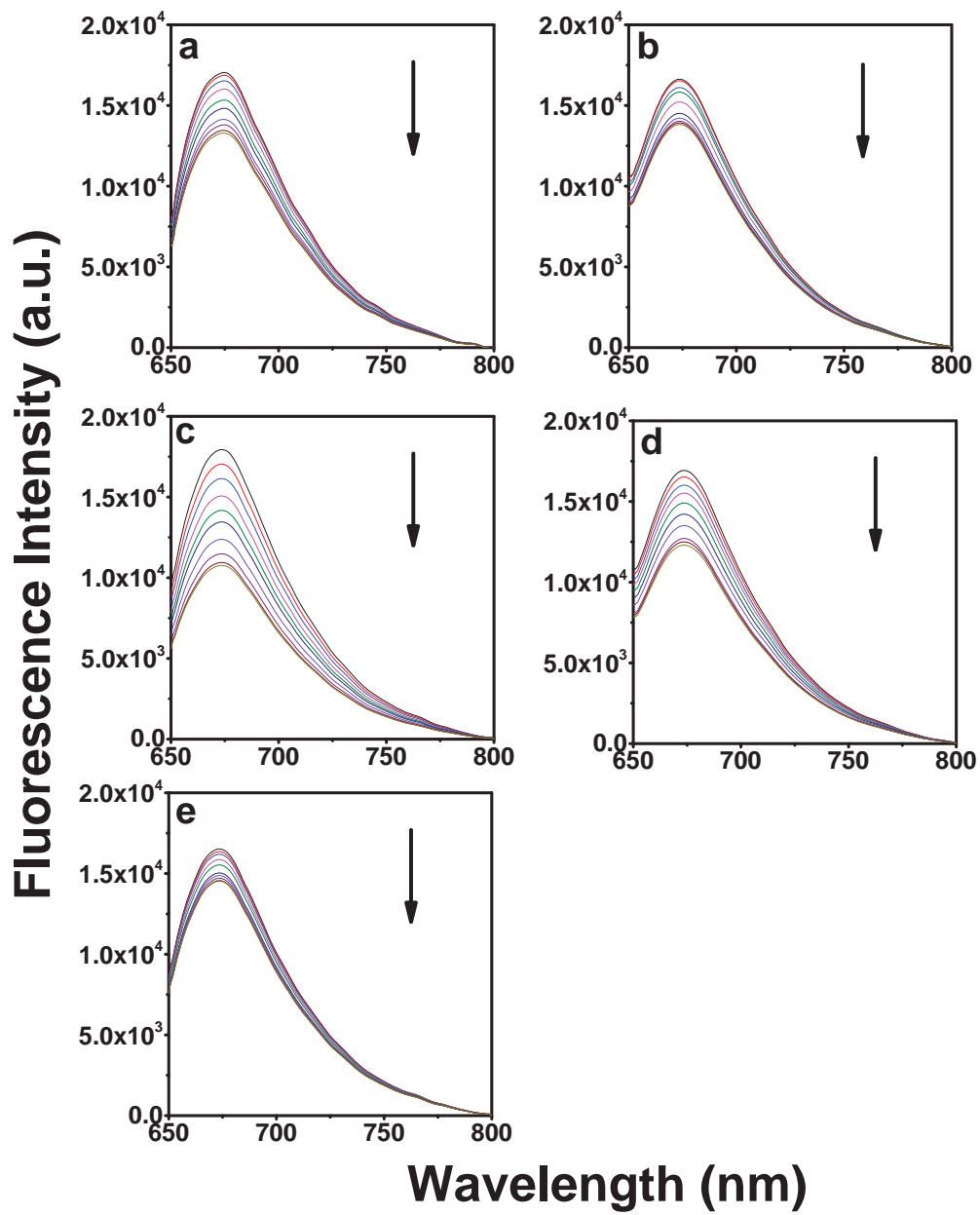


Fig. S5

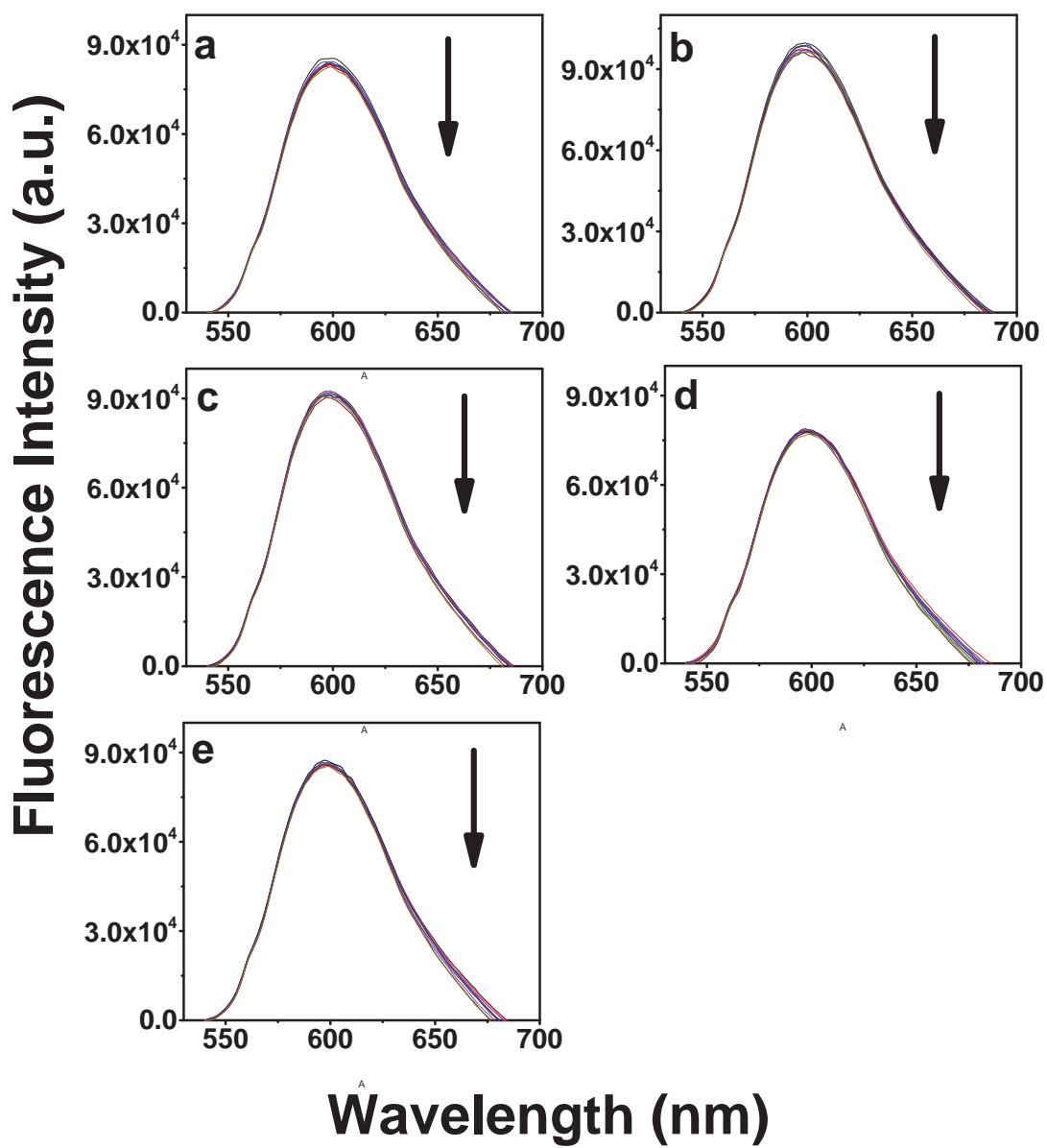


Fig. S6

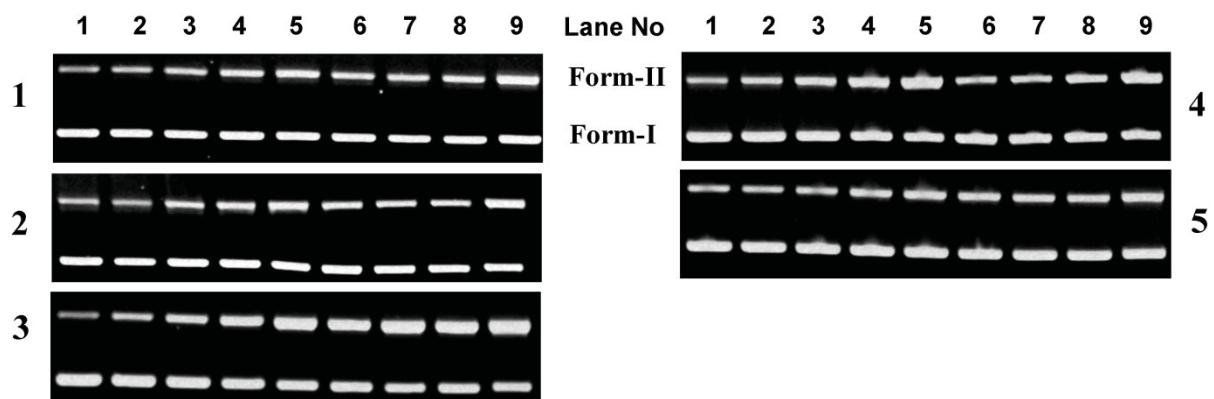


Fig. S7

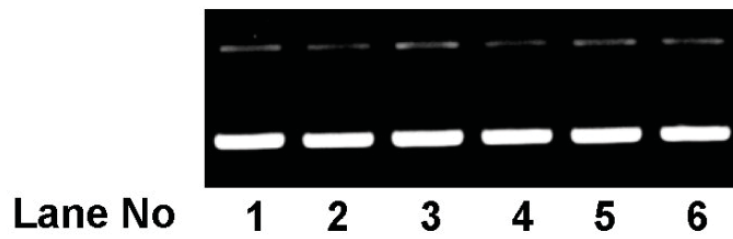


Fig. S8

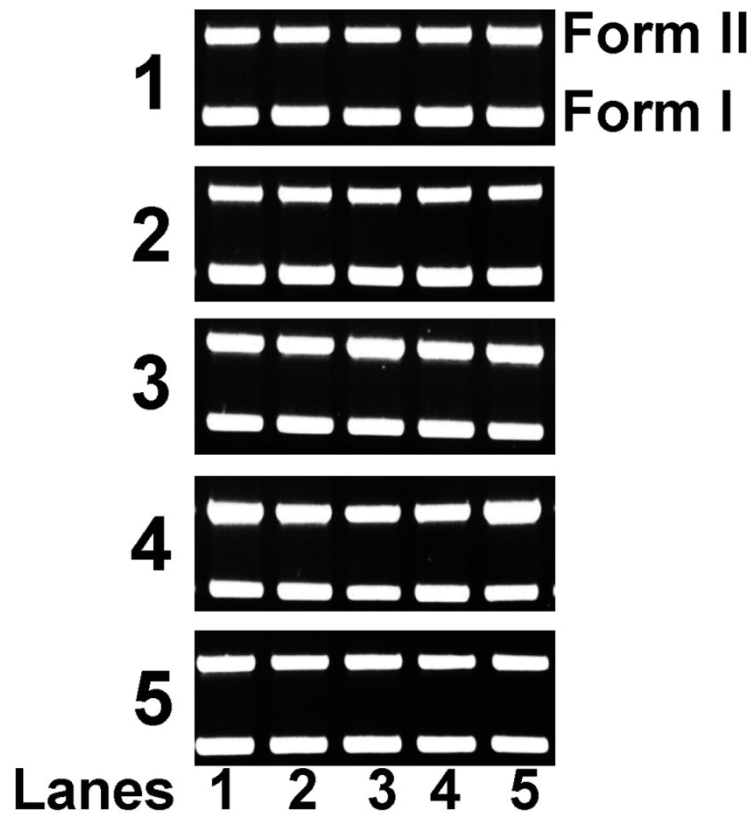


Fig. S9

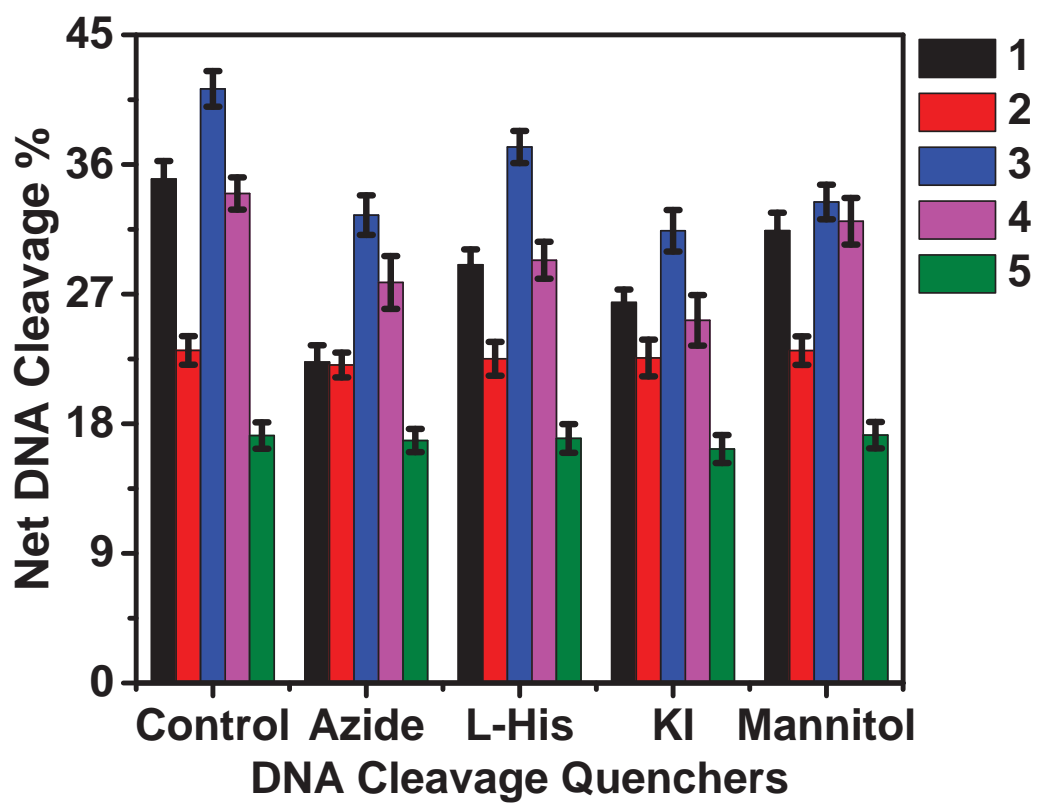


Fig. S10

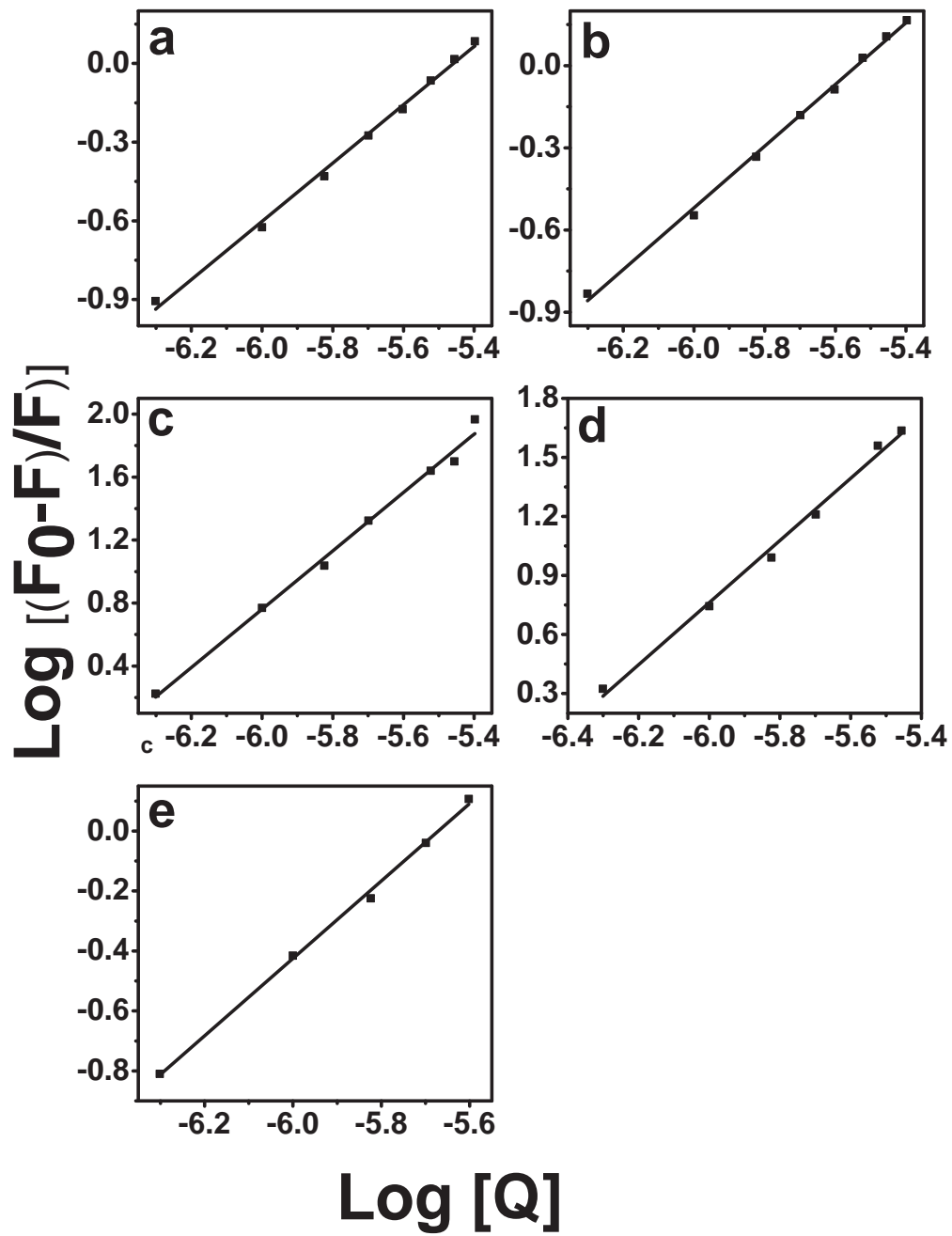


Fig. S11

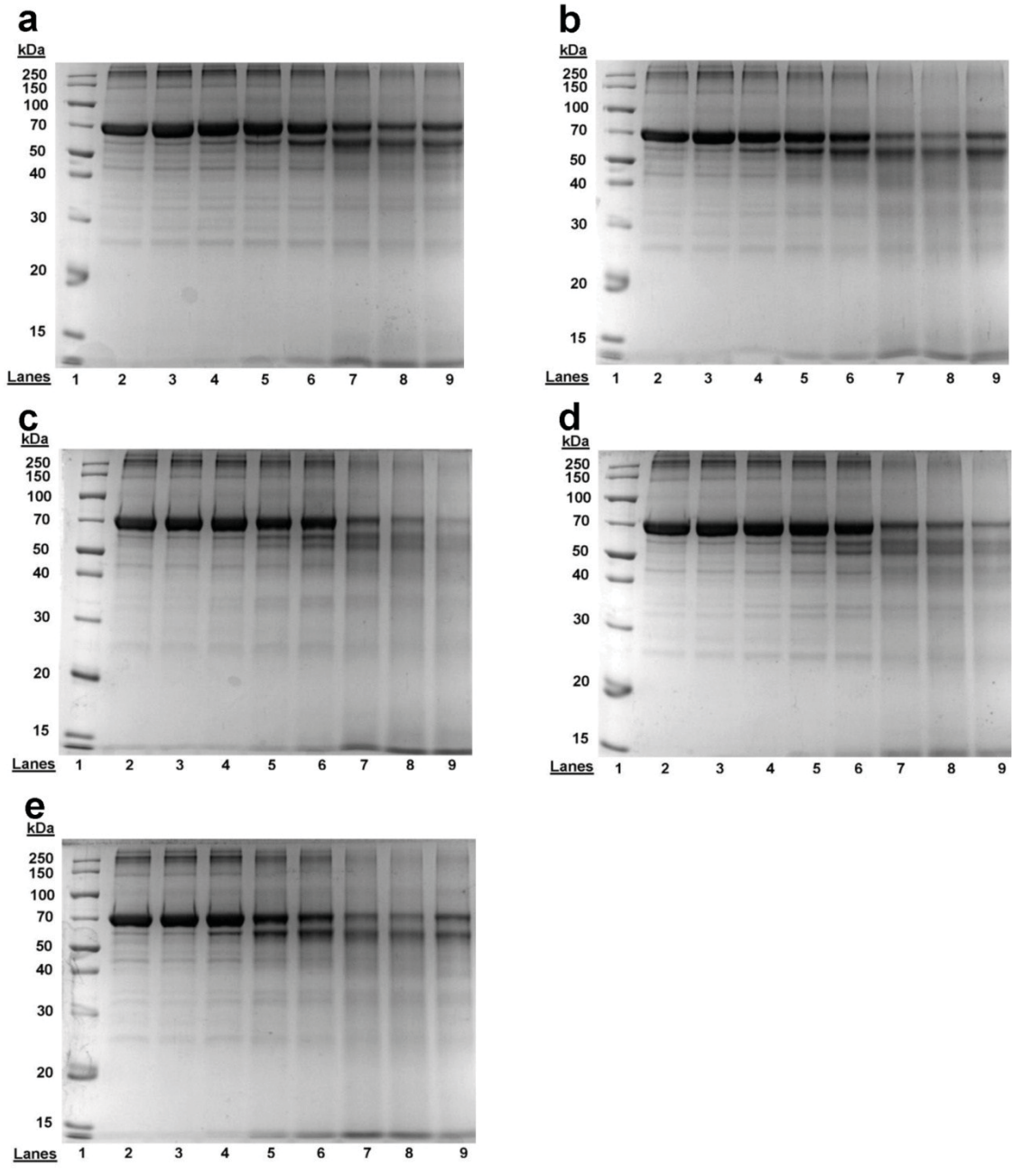


Fig. S12

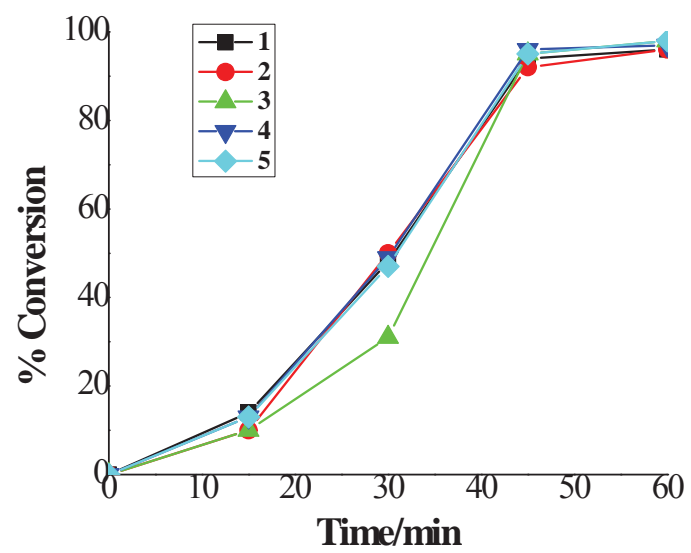


Fig. S13

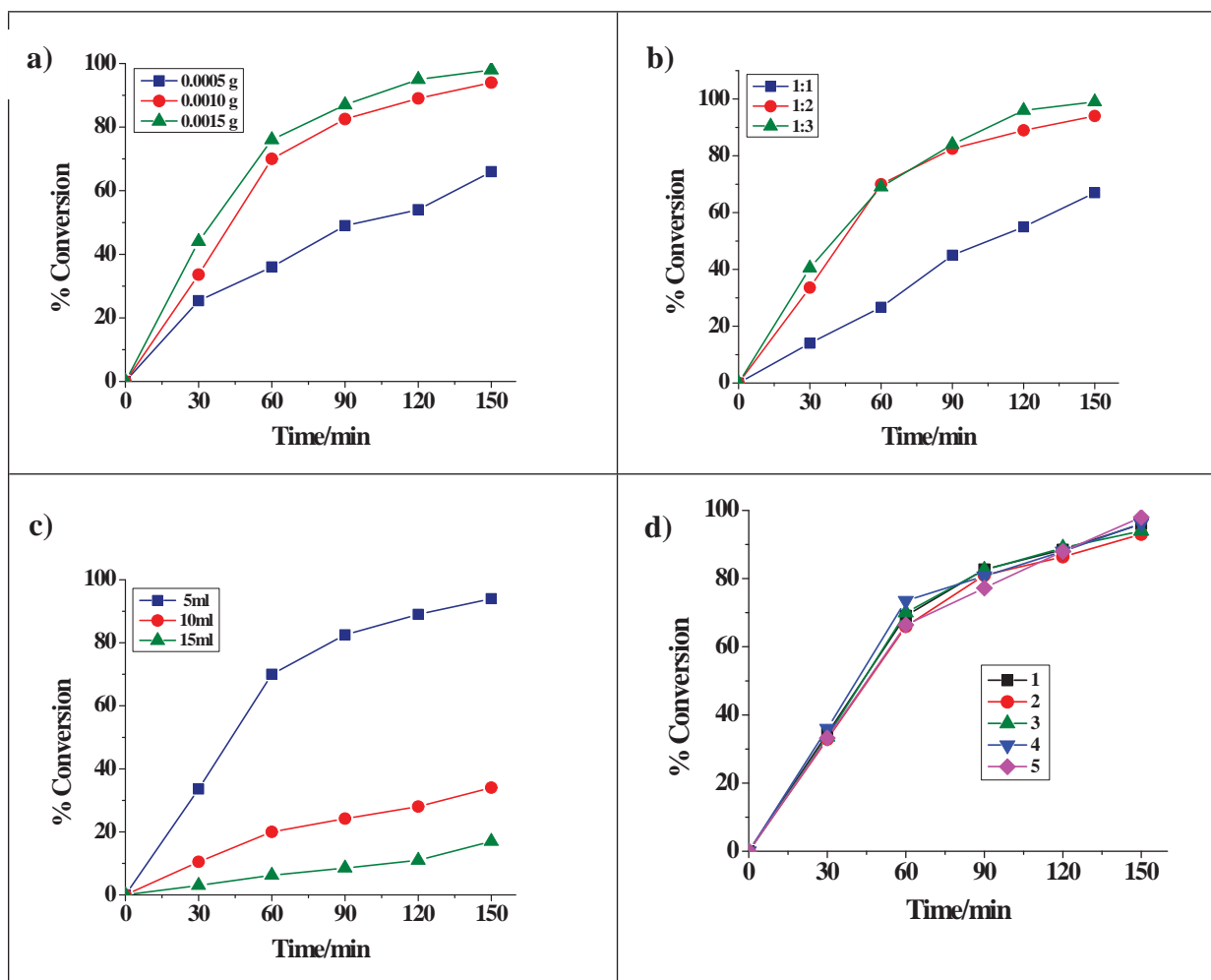


Fig. S14